Letters

Molecular Dynamics Simulations of Ligand Dissociation from Thyroid Hormone Receptors: Evidence of the Likeliest Escape Pathway and Its Implications for the Design of Novel Ligands

Leandro Martínez,[†] Paul Webb,[‡] Igor Polikarpov,[§] and Munir S. Skaf*[,†]

Instituto de Química, Universidade Estadual de Campinas - UNICAMP Cx. P. 6154, Campinas, SP 13084-862, Brazil, Diabetes Center and Department of Medicine, University of California, San Francisco, California 94122-0540, and Instituto de Física de São Carlos, Universidade de São Paulo, Av. Trabalhador São Carlense, 400, São Carlos, SP 13560-970, Brazil

Received August 12, 2005

Abstract: Steered molecular dynamics simulations of ligand dissociation from Thyroid hormone receptors indicate that dissociation is favored via rearrangements in a mobile part of the LBD comprising H3, the loop between H1 and H2, and nearby β-sheets, contrary to current models in which the H12 is mostly involved. Dissociation is facilitated in this path by the interaction of the hydrophilic part of the ligand with external water molecules, suggesting strategies to enhance ligand binding affinity.

The nuclear receptor (NR) superfamily is the largest group of ligand-dependent transactivation factors and is a major target for pharmaceutical development.[1−6] NRs are comprised of three domains: an N-terminal domain which contains a ligand-independent transactivation factor, a DNA binding domain which is responsible for target gene recognition and specificity, and a ligand binding domain (LBD) which is responsible for ligand binding, dimerization, and coregulator recruitment.

Crystallographic structures of ligand-bound NR LBDs have clarified structural features of hormone signaling via NRs.[4−8] The holo-LBD is more compact than the apo-LBD, and the ligand is generally completely buried in the core of the domain. Whereas C-terminal H12 is usually tightly packed against the core of the domain, structures of retinoic acid receptor (RAR) and the estrogen receptors revealed that C-terminal H12 can adopt different positions and led to the suggestion that H12 is mobile and acts as lid for a major route of ligand entry and release from the enclosed pocket: the mousetrap model.[9,10]

Nevertheless, the mouse-trap model remains controversial.[11,12] H12 position also influences coregulator recruitment: displacement of H12 exposes the corepressor binding surface and ligand-dependent packing of H12 against the LBD completes the coactivator binding site. Thus, the putative entry/exit route would be obstructed by corepressors in the absence of ligand and coactivator in the presence of ligand. Further, other regions of NR LBDs have been proposed to harbor ligand entry and exit routes, based on analysis of temperature factors, which provide an indirect indication of the relative mobility of different regions of the domain,[4−6] assembly assays,[12] detection of small cavities on the surface of some NR LBDs,[8] and on the basis of molecular dynamics (MD) simulations, described below.

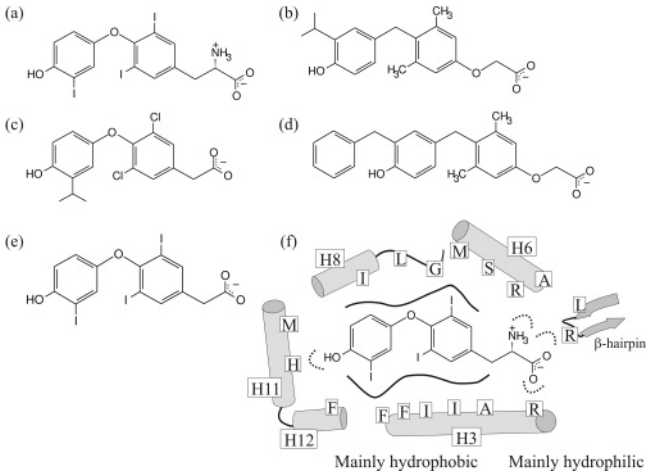

Figure 1. Structure of the ligands studied: (a) 3,5,3′-triiodo-L-thyronine (T3) and β-selective ligands (b) GC1, (c) IH5, (d) GC24, and (e) Triac. (f) Schematic representation of the binding pocket. All residues that form direct contacts with T3 in the crystal structure are indicated, according to ref 4. Most interactions with the ligand are hydrophobic, but important hydrophilic interactions are located at the extremities of the binding pocket.

Thyroid hormone receptors (TRs) mediate the biological activity of thyroid hormones.[3−6] There are two TRs which are products of two different genes, α and β, which encode at least four receptor isoforms through the process of differential RNA splicing.[4] TR X-ray structures were obtained for both α and β isoforms with natural and synthetic ligands, some of which are TRβ selective and promote reductions of serum cholesterol and rapid loss of body fat in the apparent absence of harmful effects on heart rate.[4,5,13−15] A schematic representation of the ligand binding pocket is shown in Figure 1f based on structures of T3 bound to TRs.[4] The pocket is composed mainly of hydrophobic residues which interact with the ligand core, but there are also hydrophilic residues that form hydrogen bonds and salt-bridges with either end of the ligand. TR X-ray structures, however, have provided very few clues about pathways of ligand binding and dissociation, which are governed by the dynamic behavior of the LBD.[16,17] Alternate methods are therefore required to understand these events.

Molecular dynamics simulations can provide substantial insights into ligand binding and dissociation from NRs. Schulten and co-workers have previously used a technique called steered molecular dynamics (SMD) simulations to probe dissociation of retinoic acid (RA) from its receptor.[8] The authors propose that ligand entry and exit may occur in a unidirectional fashion, in which the ligand enters the binding pocket through a mouse-trap-like mechanism (involving H12) and leaves the binding pocket through the mobile region comprising the H1−H2 loop and the β-hairpin which harbors the only discernible opening in the LBD surface. In an independent study, Karplus and co-workers used a different technique, often called locally enhanced sampling (LES) dynamics, for the same RA-RAR system and suggested that RA binds and leaves the RAR via displacement

* Corresponding author. Phone: (55) 19-3788 3093. Fax: (55) 19-3788 3023. E-mail: skaf@iqm.unicamp.br.
[†] Universidade Estadual de Campinas.
[‡] University of California.
[§] Universidade de São Paulo.

10.1021/jm050805n CCC: $33.50
Published on Web 12/02/2005

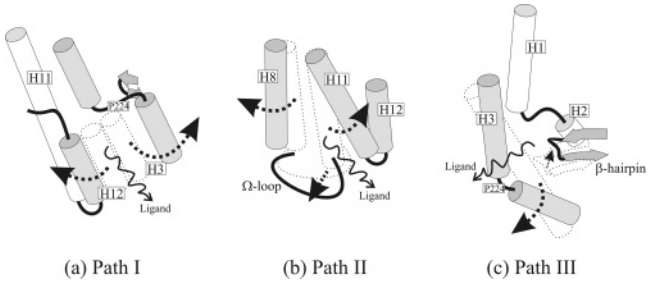

Figure 2. Main features of the three dissociation Paths: (a) Path I involves ligand dissociation through an aperture formed between H3 and H12. (b) In Path II ligands may dissociate by the separation between H8 and H11 and the retraction of the highly mobile Ω-loop. (c) In Path III, H3 is broken in two near Pro 224 and the movement of the *β*-hairpin opens the cavity through which ligands escape. Arrows indicate protein movements from ligand-bound (dashed) to unbound (solid) structures.[19]

of H12.[18] We have recently performed a large set of LES simulations to identify possible pathways of ligand release from TRs.[19] We concluded that there are three possible pathways of ligand dissociation in TRs, but their relative importance and the pertinent molecular details could not be addressed by the technique employed.[19]

In this work we report what is, to our knowledge, the largest set of molecular dynamics simulations on TRs. We performed SMD simulations to examine dissociation of the natural ligands T3 and Triac and of *β*-selective ligands GC1 and IH5 from both TRα and TR*β*, and, in addition, of GC24 from TR*β*. The structures of these ligands are represented in Figure 1. The present simulations are able to address the following questions: Which is the most favored ligand dissociation path? Why is this path favored over others? What insights does the knowledge of this path provide for the development of novel ligands of pharmacological interest?

Briefly, in SMD, a ligand is pulled out of the structural model of a given protein along routes that are chosen by the investigator. The external force is applied according to $F = k(\vec{v}t - \vec{x})$ where k and $\vec{v}$ define the stiffness and the velocity of the force, respectively, while t and $\vec{x}$ are the simulation time and displacement of the hormone from its initial position. This force is constantly modulated by the resistance that the ligand encounters: if the ligand moves forward along the pathway, $|\vec{x}|$ increases and the force decreases; if the applied force is not able to displace the ligand, F increases due to the increase in t. Thus, it is possible to obtain profiles of the force required to dissociate the ligand as a function of the simulation time and, therefore, determine how difficult it is to promote dissociation along a given path. Here, our simulated systems are composed of the TR LBD, the ligand, and a hydration shell of at least 15 Å thick around the protein plus counterions to render the system electrically neutral (approximately 54 000 atoms). Total simulation time was about 46 ns (equilibration plus 1 ns of free, NVE, dynamics, plus 1 ns dissociation simulations for each of the studied paths, for each structure). Water and ions were added with Packmol,[21] and all simulations were performed with the NAMD simulation package.[22] Further simulation details may be found in Supporting Information, and detailed descriptions of SMD and its properties can be found elsewhere.[8,23] The pulling directions $\vec{v}$ used here were chosen on the basis of our previous LES simulations (see Supporting Information),[19] which detect possible pathways of ligand dissociation without any previous assumptions.[18,19,24]

The three possible paths of ligand dissociation that we identified for TR[19] are shown in Figure 2. Path I is a variation

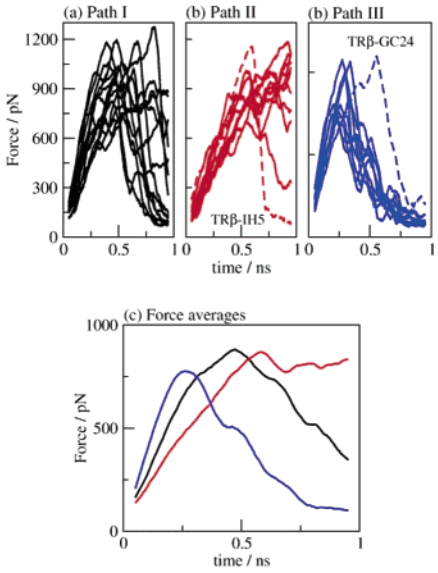

Figure 3. Force profiles for dissociation along the three paths. (a) Applied force profiles for dissociation along Path I for all simulated systems (black) show high force barriers. (b) Force profiles along Path II. The red dashed line corresponds to the force profile for the dissociation along Path II for the TR*β*-IH5 system, the only one for which dissociation along this path was observed. (c). Force profiles for Path III show lowest barriers among all simulated systems. The blue dashed line corresponds to the dissociation of the GC24 ligand from TR*β*, the only significantly different overall profile found for dissociations through Path III. (d) Averaged force profiles.

of the mouse-trap model (Figure 2a): the C-terminal H12 pulls away from the LBD allowing ligands to escape through the aperture formed between H3 and H12. Path II, observed for the first time in our previous simulation, involves part of the LBD that is known to be highly mobile: the Ω-loop between H2 and H3. Within this path, H8 and H11 dissociate from each other, and this event is accompanied by retraction of the Ω-loop to open the escape cavity (Figure 2b). Finally, Path III involves another highly mobile region of the LBD comprised of H3, the loop between H1 and H2 and nearby *β*-sheets (Figure 2c). During ligand dissociation through this path, H3 is partially disrupted in two helices around Pro 224 (TRα numbering), and the *β*-sheets move apart from H3, opening the cavity through which the ligand dissociate. Path III seems to be particularly appealing as a putative escape route in aqueous environments because it involves the unfolding of a highly hydrophilic region of the LBD.

Our simulations indicate that ligand dissociates readily along Path III and experiences significantly lower energy barriers in this path than the other two paths, irrespective of initial structure, ligand, and TR isoform. The profiles of the forces required to promote dissociation of individual ligands through Paths I−III in simulation are presented in Figure 3a−c, and averaged force profiles obtained from all simulations with each path are presented in Figure 3d. Here, increased force appears when the ligand encounters energy barriers as it begins to move out of the LBD and returns to zero as ligand leaves the LBD. Figure 3a shows that ligand dissociation along Path I was observed in 4 out of 10 SMD simulations (TR*β*-T3, TRα-IH5, TR*β*-IH5, and TR*β*-GC1). By contrast, most ligands failed to dissociate along Path II, as shown by the fact that the force profiles fail to approach zero. Here, the force increase induces protein unfolding rather than ligand release in these simulations (not shown). The sole exception was observed with the TR*β*-IH5 system, but required an abrupt breaking of hydrophobic contacts between

Table 1. Properties of the Average Force Profiles

	maximum force/pN	integrated force/pN ns
Path I	881	555
Path II	869	587
Path III	775	360

helices 8 and 11. Most strikingly, ligand dissociation was readily observed along Path III in all simulations. Furthermore, ligands experienced lower barriers as they dissociated along Path III than the other paths. As shown in Table 1, the average force along Path III reaches a maximum of 775 pN before it declines and approaches zero (Figure 3d), nearly 12% lower than the maximum observed with Path I (881 pN). For Path II, the average force reaches a plateau at ~860 pN, reflecting the fact the dissociation has not been observed along this route in most cases. The integrated forces shown in Table 1 reflect even clearer how dissociation is easiest along Path III: The total force required for the ligands to be extracted is 360 pN.ns, which is 36% smaller than in Path I (555 pN.ns) and 38% smaller than in Path II (587 pN.ns) (Integrated forces for all simulations separately are provided in Table 1, Supporting Information). These results confirm the qualitative picture that we have observed in the simulations. While dissociation through Path III was readily found on all simulations, dissociation was not observed on several simulations along the other two paths, even with different tentative pulling directions. Furthermore, pulling the ligand through Paths I and II usually rendered distortions on the secondary structure of the protein, while dissociation through Path III is smooth and required gentle protein movements.

Why is ligand dissociation through Path III easier than along the other paths? Part of the explanation is probably related to the fact that ligand escapes through a highly mobile region of the protein, as demonstrated by the temperature factors in crystallographic models.[4,5,13,15,20] However, this cannot be the sole explanation: Ligand release along Path II involves another highly mobile region of the protein (the Ω-loop) and yet is not favored.

To gain insights into this phenomenon, we computed the interaction energies of the ligand with the whole environment (protein + water + counterions) during dissociation. Figure 4 shows the profiles of Lennard−Jones (vdW) and electrostatic interactions as functions of simulation time for the systems considered here and for which dissociation through Path I was observed. The electrostatic interaction between ligand and the whole environment passes through a local maximum (less attractive, unfavorable barrier) during dissociation through Path I. In contrast, dissociation through Path III occurs with a steady increment of the electrostatic attractive interactions. This is because, in Path III, the polar groups of the ligands dissociate directly into the aqueous environment (see Figures 1e and 2c). For T3, the hydrogen bonds and electrostatic interactions that the carboxylate and amine groups form with the residues in the binding pocket are smoothly substituted by nearly equally strong hydrogen bonds with water molecules in the protein exterior. By contrast, for ligand dissociation to occur through Paths I and II, these polar groups must cross the hydrophobic pocket, while losing most of the electrostatic (attractive) interactions. Interaction of waters with the polar head of the ligand during dissociation has also been observed for the dissociation of the retinoic acid from its receptor in SMD simulations.[8] The fact that other NR ligands display similar polarity to TR ligands and are positioned in a similar fashion in their respective pockets suggests that this pathway represents a plausible mechanism

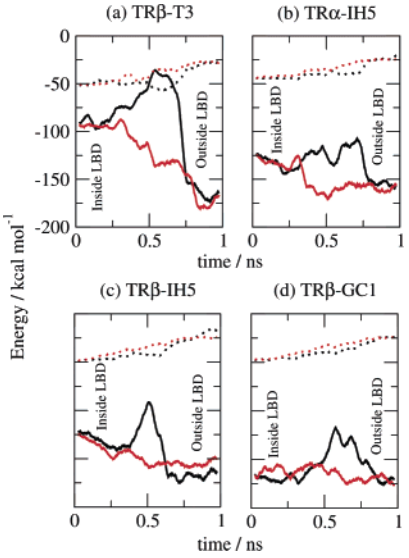

Figure 4. Electrostatic (solid lines) and dispersive (dotted lines), vdW interaction energies of the ligand with the whole environment during dissociation through Path I (black) and Path III (red). There is no significant difference for vdW interactions between the two paths. An excess barrier of at least 40 kcal mol^{-1} of electrostatic energy must be overcome during dissociation through Path I relative to Path III because the hydrophilic head of the ligand must cross the hydrophobic pocket during dissociation along route I. This effect is even more important for T3 dissociation because of the highly polar head present in this ligand.

for the dissociation of many other NR ligands from their respective LBDs.[1−13]

What are the implications of the present conclusions to the development of novel TR ligands? First, we propose that strategies that increase the hydrophilicity of the polar head of the ligand would not increase ligand binding affinity. While such modifications would reinforce the interactions with the polar amino acid residues of the binding pocket, they would also enhance interactions with water molecules outside the LBD and, hence, favor dissociation. We believe that the polar head of the ligands are important for determining the orientation of the ligand inside the binding pocket, but increased polarity should not necessarily promote higher binding affinities. Indeed, the natural ligands T3 and T4 have both a carboxylate and an amino group, but several ligands lacking the amino group (and, therefore, having less polar heads), such as the natural hormone Triac and synthetic ligands GC1, GC24, and IH5, bind the LBD with high affinity.[4−7] Even substitution of the ether and carboxylate groups of GC1 (Figure 1b) by a neutral hydroxyethil (CH_2CH_2OH) group provides ligands with high affinity.[25] Therefore, we propose that the best strategy to develop novel high affinity TR ligands is to concentrate on increasing the interactions of the groups around the phenolic ring of the ligands with their protein environment. This proposal is supported by the exceptional profile observed for GC24 dissociation through Path III (blue dashed line in Figure 3c, integrated force: 562 pN.ns). Here, a significant increase in the force is necessary to obtain dissociation along Path III relative to other ligands, resembling the profiles for Path I. This is because the GC24 ligand (Figure 1d) has a benzene ring that strongly interacts with nonpolar residues between H3 and H12, as seen in the crystallographic structure[5] (see Figure 1e). This hydrophobic, aromatic interaction in the opposite end of the ligand, results in higher dissociation barriers. Introduction of more localized hydrophilic interactions in this region should also have similar effects without the introduction of steric hindrance for ligand

entry. This view is supported by the recent ligand screening performed at Pfizer labs, where it was observed that the removal of the phenolic group in T3 analogues decreases the binding affinity of the ligands by 2 orders of magnitude.[26] In the context of the present work, we interpret this result by noting that elimination of the phenolic group represents the loss of an important hydrophilic interaction that is not replaced by ligand−solvent interactions during dissociation through Path III.

In summary, our results show that the likeliest route for ligand dissociation from TR involves the highly mobile region at the bottom of the LBD comprising part of H3, the loop between H1 and H2, and nearby β-sheets, and that this mechanism is favored by the replacement of hydrophilic interactions of the polar end of the ligand with the protein by ligand−water (external) interactions. Further analysis suggests that effective strategies for developing novel, high affinity, TR ligands should concentrate on increasing the interactions in the region of the ligands phenolic rings with the protein environment, as opposed to increasing the polarity in the carboxylate end of the ligand. We hope that these insights will be useful for rational ligand development aimed at TRs and other NRs.

Acknowledgment. The authors thank the Brazilian agencies FAPESP (03/09361-4 to M.S and 99/03387-4 to I.P) and CNPq (401913/2003-1 to M.S.) for financial support.

Supporting Information Available: Methodological details, ligand parameters, topologies, and integrated forces for individual simulations. This material is available free of charge via the Internet at http://pubs.acs.org.

References

(1) McKenna, N. J.; O'Malley B. W. Combinatorial control of gene expression by nuclear receptors and corregulators. *Cell* **2002**, *108*, 465−474.
(2) Pelton, P. D.; Patel, M.; Demarest, K. T. Nuclear receptors as potential targets for modulating reverse cholesterol transport. *Curr. Top. Med. Chem.* **2005**, *5*, 265−281.
(3) Cheng, S. Thyroid hormone receptor mutations and disease: beyond thyroid hormone resistance. *Trends Endocrin. Met.* **2005**, *16*, 176−182.
(4) Wagner R. L.; Huber R. B.; Shiau, A. K.; Kelly, A.; Lima, S. T. C.; Scanlan, T. S.; Apriletti, J. W.; Baxter, J. D.; West, B. L.; Fletterick, R. J. Hormone Selectivity in Thyroid Hormone Receptors. *Mol. Endocr*. **2001**, *15*, 398−410.
(5) Borngraeber, S.; Budny, M. J.; Chiellini, G.; Lima, S. T. C.; Togashi, M.; Webb, P.; Baxter, J. D.; Scanlan, T. S.; Fletterick, R. J. Ligand selectivity by seeking hydrophobicity in thyroid hormone receptors. *Proc. Natl. Acad. Sci. U.S.A.* **2003**, *100*, 15358−15363.
(6) Webb, P. Selective activators of thyroid hormone receptors. *Expert. Opin. Inv. Drug.* **2004**, *13*, 489−500.
(7) Togashi, M.; Borngraeber S.; Sandler, B.; Fletterick, R. J.; Webb, P.; Baxter, J. D. Conformational adaptation of nuclear receptor ligand binding domains to agonists: Potential for novel approaches to ligand design. *J. Steroid Biochem.* **2005**, *93*, 127−137.
(8) Kosztin, D.; Izrailev, S.; Schulten, K. Unbinding of Retinoic Acid from its Receptor Studied by Steered Molecular Dynamics. *Biophys. J.* **1999**, *76*, 188−197.
(9) Bourget, W.; Ruff, M.; Chambon, P.; Gronemeyer H.; Moras D. Crystal structure of the ligand-binding domain of the human nuclear receptor RXR-α. *Nature* **1995**, *375*, 377−382.
(10) Renaud, J. P.; Rochel, N.; Ruff, M.; Vivat, V.; Chambon, P.; Gronemeyer, H.; Moras, D. Crystal structure of the RAR-α ligand-binding domain bound to all-*trans* retinoic acid. *Nature* **1995**, *378*, 681−689.
(11) Nettles, K. W.; Greene, G. L. Ligand control to coregulator recruitment to nuclear receptors. *Ann. Rev. Physiol.* **2005**, *67*, 309−333.
(12) Pissios, P.; Tzameli, I.; Kushner P. J.; Moore, D. D. Dynamic Stabilization of Nuclear Receptor Ligand Binding Domains by Hormone or Corepressor Binding. *Mol. Cell* **2000**, *6*, 245−253.
(13) Wagner, R. L.; Aprietti, J. W.; McGrath, M. E.; West, B. L.; Baxter, J. D.; Fletterick, R. J. A structural role for hormone in the thyroid hormone receptor. *Nature* **1995**, *378*, 690−697.
(14) Ye, L.; et al. Thyroid Receptor Ligands. 1. Agonist Ligands Selective for the Thyroid Receptor β1. *J. Med. Chem.* **2003**, *46*, 1580−1588.
(15) Nunes, A. M.; et al. Crystallization and preliminary X-ray diffraction studies of isoform α1 of the human thyroid hormone receptor ligand-binding domain. *Acta Crystallogr. D* **2004**, *60*, 1867−1870.
(16) Gee, A. C.; Katzenellenbogen, J. A.; Probing conformational changes in the estrogen receptor: evidence for a partially unfolded intermediate facilitating ligand binding and release. *Mol. Endocr.* **2001**, *15*, 421−428.
(17) Kallenberger, B. C.; Love, J. D.; Chatterjee, V. K.; Schwabe, J. W.; A dynamic mechanism of nuclear receptor activation and its perturbation in human disease. *Nat. Struct. Biol.* **2003**, *10*, 136−140.
(18) Blondel, A.; Renaud, J. P.; Fischer, S.; Moras, D.; Karplus, M.; Retinoic Acid Receptor: a simulation analysis of retinoic acid binding and the resulting conformational changes. *J. Mol. Biol.* **1999**, *291*, 101−115.
(19) Martínez, L.; Sonoda, M. T.; Webb, P.; Baxter, J. D.; Skaf, M. S.; Polikarpov, I. Molecular Dynamics Simulations Reveal Multiple Pathways of Ligand Dissociation from Thyroid Hormone Receptors. *Biophys. J.* **2005**, *89*, 2011−2023.
(20) Nunes, F. M.; Aparicio, R.; Santos, M. A. M.; Portugal, R. V.; Dias, S. M. G.; Neves, F. A. R.; Simeoni, L. A.; Baxter, J. D.; Webb, P.; Polikarpov, I. Crystallization and preliminary X-ray diffraction studies of isoform alpha 1 of the human thyroid hormone receptor ligand-binding domain. *Acta Crystallogr. D.* **2004**, *60*, 1867−1870.
(21) Martínez, J. M.; Martínez, L. Packing optimization for the automated generation of complex system's initial configurations for molecular dynamics and docking. *J. Comput. Chem.* **2003**, *24*, 819−825. (http://www.ime.unicamp.br/∼martinez/packmol).
(22) Kalé, L.; Skeel, R.; Bhandarkar, M.; Brunner, R.; Gursoy, A.; Krawetz, N.; Phillips, J.; Shinozaki, A.; Varadarajan, K.; Schulten, K. NAMD2: Greater scalability for parallel molecular dynamics. *J. Comput. Phys.* **1999**, *151*, 283−312.
(23) Isralewitz, B.; Baudry, J.; Gullinsgrud, J.; Kosztin, D.; Schulten, K. Steered molecular dynamics investigations of protein function. *J. Mol. Graph.* **2001**, *19*, 13−25.
(24) Elber, R.; Karplus, M.; Enhanced sampling in molecular dynamics: use of time-dependent Hartree approximation for a simulation of carbon monoxide diffusion through myoglobin. *J. Am. Chem. Soc.* **1990**, *112*, 9161−9175.
(25) Ye, H. F.; O'Reilly, K. E.; Koh, J. T. A Subtype-Selective Thyromimetic Designed to Bind a Mutant Thyroid Hormone Receptor Implicated in Resistance to Thyroid Hormone. *J. Am. Chem. Soc.* **2001**, *123*, 1521−1522.
(26) Dow, R. L.; et al. Discovery of a Novel Series of 6-Azauracil-Based Thyroid Hormone Receptor Ligands: Potent, TRβ Subtype Selective Thyromimetics. *Bioorg. Med. Chem. Lett.* **2003**, *13*, 379−382.

JM050805N